



	<b>Experiment title:</b> Metamagnetic transition in size-selected FeRh B2 nanocrystal	<b>Experiment number:</b> HC-4794
<b>Beamline:</b> ID12	<b>Date of experiment:</b> from: 24 May 2022 to: 30 May 2022	<b>Date of report:</b> 26 July 2022
<b>Shifts: 18</b>	<b>Local contact(s):</b> Fabrice WILHELM	<i>Received at ESRF:</i>
<b>Names and affiliations of applicants</b> (* indicates experimentalists): <b>Main proposer:</b> DUPUIS Véronique* (Laboratory UCB Lyon 1 - CNRS UMR 5306 Institut Lumière Matière (iLM) Domaine scientifique de La Doua, 6 rue Ada Byron FR – 69622 VILLEURBANNE Cedex) <b>Co-Proposers and experimentalists:</b> HERRERA Guillermo*, TOURNUS Florent * and LE-ROY Damien (iLM)		

## Report:

### Scientific background :

Near equiatomic composition, FeRh bulk alloys exhibit a CsCl-type (B2) chemically ordered phase related to a metamagnetic transition from an antiferromagnetic (AFM) to a ferromagnetic (FM) state close to ambient. This first order metamagnetic transition is generally interpreted in terms of the collapse of induced Rh magnetic moment at low temperature. The objective of this proposal is to **study thermally driven chemical order transition and magnetism in bi-metallic FeRh nanoalloys**. To reach this purpose, X-ray absorption spectroscopy and magnetic circular dichroism (**XAS/XMCD**) **experiments on ID12** have been performed at both Fe K-edges and Rh L-edges on **as-prepared and annealed** FeRh nanoparticles (NPs) deposited on Silicon or SrTiO<sub>3</sub> (STO) substrate with or without carbon capping before transfer in air. These results will allow us to describe **local structural and magnetic evolution for each specific element as a function of FeRh clusters size, density and substrates**.

### Sample preparation and Characterization

FeRh clusters were produced in gas phase with two different diameters 3 and 7 nm by Mass-Selected Low Energy Cluster Beam Deposition (MS-LECBD) in UHV chamber on different substrates. While as-prepared NPs are in the chemically disordered fcc A1 phase with a paramagnetic like-behaviour, UHV annealing around 900K leads systematically to chemical ordering for FeRh nanocrystal towards the B2 phase with strong magnetic signature. Notice that Epitaxy has been recently observed on thin film of mass-selected FeRh clusters (in the 3-10 nm range in diameter) deposited on STO substrate (see experimental report A32-3-745 on BM32 beamline) while thick FeRh nanogranular sample (with diameter greater than 30 nm) present a broad metamagnetic transition with applied magnetic field dependence for transition temperature and a global few tens per cent of residual magnetization at low temperature (unpublished SQUID magnetometry measurements).

### Experimental results

Preliminary XANES Measurements have been performed on a dozen of samples in Fluorescence and Total electron yield at both Fe K-edges (7.13 keV with HE 52 undulator) and Rh L-edges (3.14 keV with HE 38 undulator) by using normal, grazing incidence and Silicon Drift Detector (no filter) in view to optimize experimental conditions to extract significant XMCD signal from our various bimetallic nanostructures.

For all the samples, we systematically found that Fluorescence signal is better in grazing incidence (10-20°) than in normal configuration to avoid Bragg peaks from substrates but also from B2 large nanocrystallites in annealed 150nm-thick FeRh samples. Moreover the XAS signal is strongly improved by using the SDD detector as background decrease given the low quantity of absorbing atoms, especially for our thin samples with a few nm of equivalent FeRh thickness.

Here, we report comparative XAS/XMCD results obtained for 3 couples of samples mounted on a specific 15° incidence sample holder in the vacuum cryomagnet chamber (up to 7 T in the 3k-320K temperature range):

- **Thick FeRh NPs samples on Si** protected with C-capping (equivalent FeRh NPs thickness of 150 nm) TM1623 (annealed sample at 700°C) to compare to TM2121 (as-prepared sample)
- **Thin FeRh NPs with 7 nm in diameter on Si** with C-capping (equivalent FeRh thickness of 3 nm) TM1639 (annealed sample at 700°C) and TM2219 (as-prepared sample)
- **Thin FeRh NPs with 3 nm in diameter on STO** (equivalent FeRh thickness of 1nm) TM2109 (annealed sample at 600°C with C-capping) and TM2127 (annealed at 800°C without C-capping)

First of all, we clearly obtained two different metallic XANES/XMCD signatures at the Rh-L<sub>2,3</sub> edges for all as-prepared and annealed samples as-illustrated on the figure 1. Moreover, we clearly identify XANES at Fe-K edge change from A1 fcc to B2 (bcc-like Fe) upon annealing for samples deposited on silicon substrates (see Fig. 2). Unfortunately, spectrums at Fe-K edge are unexploitable for samples deposited on STO substrate due to a strong Ti K-edge absorption background.

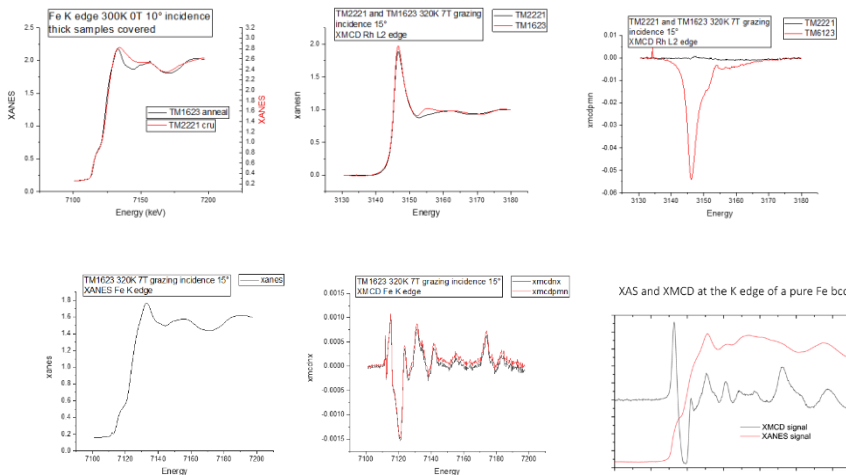


**Fig. 1:** XANES at Fe-K and Rh L<sub>2</sub>-edges on as-prepared (TM221 in red) and annealed (TM1623 in black) 150nm-thick FeRh NPs sample on Si with C-capping with the corresponding XMCD signal at 320 K and 7T at Rh edge.

**Fig. 2:** XANES/XMCD 320 K and 7T on annealed (TM1623) at Fe-K edge compared to Fe foil [ref 1].

On the annealed Thick FeRh sample (TM1623) on Si substrate, we have been able to follow the metamagnetic AFM/FM transition in the range of temperature 3-320 K by recording thermal XMCD signal at the Rh L<sub>2</sub>-edge for a constant magnetic field of 7 T, in the heating and cooling mode. On Figure 3, we clearly see a non-zero residual magnetization for Rh at low temperature. Notice that the existence of a metastable FM high-volume state in which Rh having a local magnetic moment at low temperature, has been theoretically predicted [ref. 2].

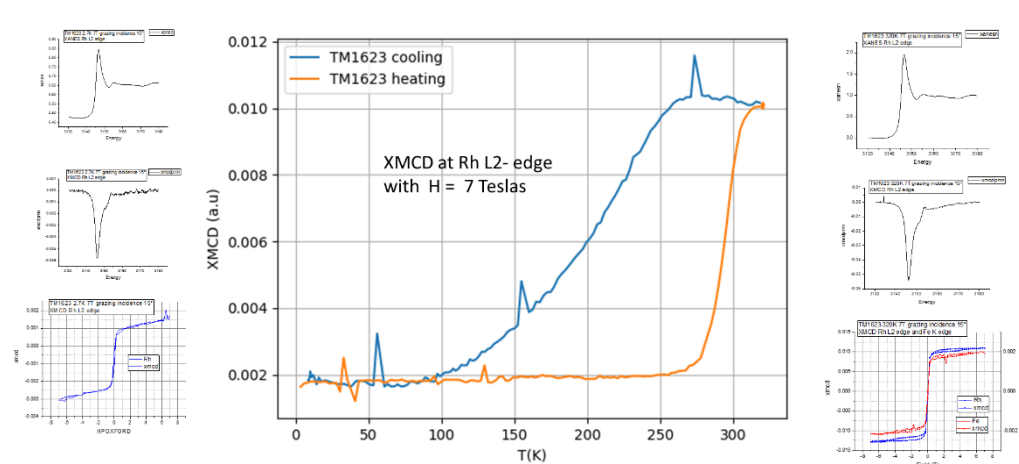


**Fig. 3:** Thermal XMCD evolution at Rh L<sub>2</sub> edge on annealed (TM1623) with the corresponding XANES/XMCD and hysteresis loop recorded at 2.7 K (left) and at 320 K (right side).

For thin FeRh NPs samples on Si substrate, even if we obtained a clear B2 structure after 700°C-annealing at both Fe K-edge and Rh L-edge, we confirm that the AFM/FM is completely overridden with strong FM exchange interactions between Rh and Fe at all temperatures (see Fig. 4). This behavior is probably related to finite size relaxation effects which avoid AFM coupling between nearest neighbors iron sites, even for initial FeRh NPs diameter as large as 7nm. [ref.3]

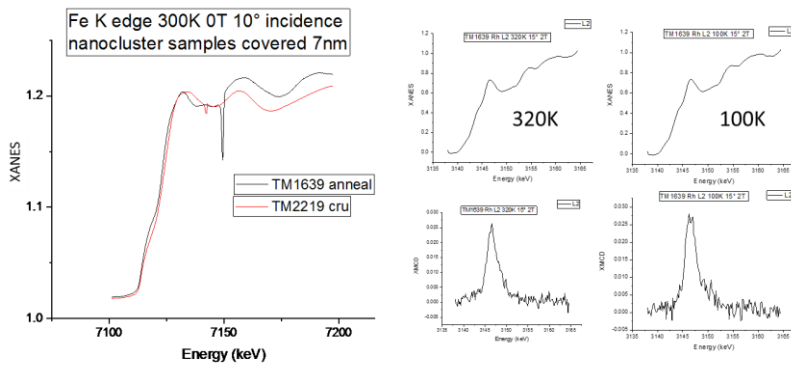


**Fig. 4:** XANES at Fe-K and Rh  $L_2$ -edges on as-prepared (TM2219 in red) and annealed (TM1639 in black) 3nm-thin FeRh NPs sample on Si with C-capping with the corresponding XMCD signal at 320 K and 100K under 2T at Rh edge.

For FeRh NPs with 3 nm in diameter in epitaxy on perovskite oxide monocrystals, due to the strong absorption at Ti K-edge (4966 keV) which is before the Fe-K edge (7.113 keV), only XANES at the Rh  $L_{2,3}$  edges (equal to 2.995 and 3.139 keV) are usable. XMCD at Rh  $L_2$ -edge, reveal the same magnetic behavior as for previous thin samples on Si. Meaning that despite epitaxy between metallic NPs and STO, strains at the interface seem to be not sufficient to counter balance strong FM exchange interactions between Rh and Fe at all temperatures. Note that low temperature photoluminescence effects in grazing incidence and total fluorescence detection mode have been observed at  $3K < T < 50K$ , for oxygen-deficient post-annealed samples at  $T < 800^\circ C$  on STO substrates.

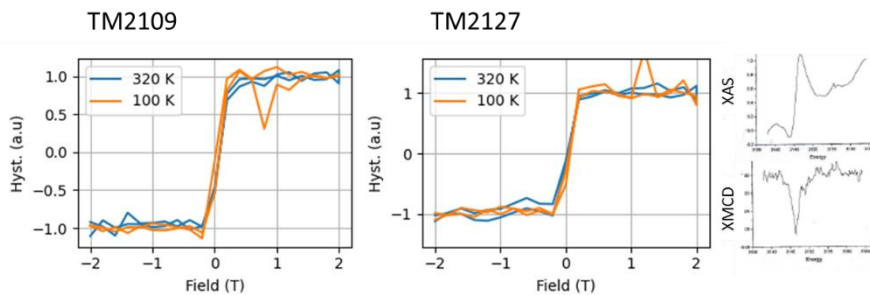


**Fig. 5:** Hysteresis loop at Rh  $L_2$ -edges on thin film of FeRh NPs with 3 nm in diameter on STO substrate (equivalent FeRh thickness of 1nm) TM2109 (annealed sample with C-capping) and TM2127 (annealed sample without C-capping) with the corresponding XMCD signal at 100K under 2T at Rh edge.

As a conclusion, this present study clearly underlines the main role of Rh atoms on the metamagnetic transition for high density FeRh NPs samples while for lower densities samples, further inquiries would require both the use of quarter-wave plate to enhance the circular polarization rate and Silicon Drift detector with appropriate energy filter mounted in the 8T-cryomagnet to improve the signal to noise ratio of XAS/XMCD.

## REFERENCES

- <sup>1</sup> O. Mathon, F. Baudalet, J-P Itie, S. Pasternak, A. Polian and S. Pascarelli, J. Synchrotron Rad. 11, 423-427 (2004)
- <sup>2</sup> L. Moruzzi and P. M. Marcus, Phys. Rev. B 46, 2864 (1992)
- M. E. Gruner, E. Hoffmann, and P. Entel, Phys. Rev. B 67, 064415 (2003)
- <sup>3</sup> G. Herrera, A. Robert, V. Dupuis, N. Blanchard, O. Boisson, C. Albin, L. Bardotti, D. Le Roy, F. Tournus and A. Tamion, Eur. Phys. J. Appl. Phys. 97, 32 (2022)